

# NEURAL-NETWORK-BASED ALGORITHMS OF HYDRAULIC ROUGHNESS FOR OVERLAND FLOW

C. J. Lopez-Sabater, K. G. Renard, V. L. Lopes

**ABSTRACT.** *This study presents a series of algorithms developed to estimate hydraulic roughness coefficients for overland flow. The algorithms are combinations of neural networks that use surface configuration parameters and the local flow Reynolds number as inputs, and provide an estimate of the roughness coefficient (Darcy-Weisbach, Manning, or Chezy). Results presented here show that as new neural networks are combined into the stacked algorithm, the estimate errors become gradually smaller. The Final Prediction Error index has been used to identify the optimum network size. Additionally, the dataset used to develop the neural networks, developed from measurements taken at approximately equal Reynolds number intervals, has been found to benefit the algorithms predicting Chezy coefficients. The scarcity of data points in some regions of the output space for the Darcy-Weisbach and Manning models caused a reduction in the predictability of the algorithms for these regions and prevented the use of more complex neural networks. The algorithms have been tested for a wide range of input variables in a detailed sensitivity analysis and have produced reasonable results in all cases.*

**Keywords.** *Overland flow, Hydraulic roughness, Mathematical models, Neural networks.*

The resistance to overland flow offered by the surface of a hillslope may be expressed using hydraulic roughness coefficients. In one of the earliest studies on overland flow hydraulics, Emmett (1970) described the roughness coefficients of field plots as consisting of two components: particle roughness, associated with the effects of single sand grains, gravel, and plant sprouts; and form roughness, representing the effect of microtopographic irregularities. In a laboratory experiment, Rauws (1988) also described hydraulic roughness coefficients as the sum of grain and form components, their contribution to the total friction being strongly variable and depending upon the Reynolds number and flow depth. Abrahams et al. (1990) concluded from a series of experiments on semiarid grassland and shrubland hillslopes that hydraulic roughness coefficients are related to the Reynolds number, and that the trend of this relationship depends on the surface properties and shape.

Overland flow generally occurs as a discontinuous shallow sheet of water with threads of flow diverging and converging around microtopographic elevations, rocks, and vegetation. As a result, flow depths and velocities, as well as infiltration rates, are highly variable in space and time. In the past, hillslope and watershed runoff simulations have been

performed using primarily one-dimensional numerical models. These models represent complex surfaces as planes with constant hydraulic properties and do not explicitly account for microtopography and spatially variable soil properties within the planes. The model coefficients then become fitting parameters requiring calibration data, and predictions are consequently difficult. In recent years, two-dimensional overland flow models have become common (Fiedler and Ramirez, 2000; Gandolfi and Savi, 2000; Govindaraju et al., 1992; Zhang and Cundy, 1989). The detailed scale at which two-dimensional models work allows them to explicitly account for spatial variations in hillslope physical characteristics, including surface roughness, infiltration, and microtopography. However, none of these models has yet considered the spatial and temporal variability of roughness coefficients.

When theoretical modeling is difficult, empirical, data-driven modeling provides a useful alternative. In recent years, artificial neural networks have been proposed as promising tools for developing empirical models in many disciplines of science and engineering (e.g., Schaap et al., 1998; Shayya and Sablani, 1999). Lopez-Sabater (2001) tested different neural-networks to predict hydraulic roughness coefficients using a variety of surface parameters, the surface slope, and the flow Reynolds number as input variables. The approach followed in his study was to consider a number of candidate networks, and to select the network that best predicted the roughness coefficients. The selected neural networks were successfully used to reproduce roughness coefficients obtained from a flume experiment. However, when the networks were used to estimate roughness coefficients for input values that were within the range, but slightly different from those contained in the dataset, the predicted coefficients were sometimes out of the expected range.

One of the reasons used to explain the anomalous behavior of the neural networks was that a single neural network might not be able to extract all the information from the dataset that

---

Article was submitted for review in May 2001; approved for publication by the Soil & Water Division of ASAE in March 2002.

The authors are Carlos J. Lopez-Sabater, ASAE Student Member, Graduate Student, University of Arizona, Department of Agricultural and Biosystems Engineering, Tucson, AZ; Kenneth G. Renard, ASAE Member Engineer, Adjunct Professor, Dept. of Agricultural and Biosystems Engineering; and Vincente L. Lopes, Associate Professor, School of Renewable Natural Resources, University of Arizona, Tucson, Arizona. Corresponding author: Carlos J. Lopez-Sabater, Department of Agricultural and Biosystems Engineering, University of Arizona, Tucson, AZ 85721; phone: 520-621-3691; fax: 520-621-3963; e-mail: clopez@westconsultants.com; cjsl@mixmail.com.

was used to calibrate it. Using a single optimal model implicitly assumes that one neural network can extract all the information available from the dataset and that other candidate networks are redundant. However, there is no assurance that any individual network extracts all relevant information from the dataset. Some authors have suggested that combining multiple neural networks in stacked models leads to a higher forecast accuracy (Martin and Morris, 1999; Sridhar et al., 1996). The idea of combining neural networks capture different aspects of the dataset, and that aggregating this information should reduce uncertainty and provide more accurate predictions.

The objective of this research was to develop improved algorithms to predict hydraulic roughness coefficients. The algorithms are based on the concept of stacked neural networks and use selected surface configuration parameters and the local flow Reynolds number as input variables. The algorithms can then be used, in conjunction with two-dimensional overland flow models, to estimate roughness parameters for each computation node and time step in a numerical simulation. The procedure can also be useful for one-dimensional applications in which conditions across the flow direction are approximately homogeneous, as in the case of border irrigation.

## MATERIALS AND METHODS

### EXPERIMENT

A laboratory experiment was performed to produce a large dataset that could be used to train neural networks in the prediction of hydraulic roughness coefficients. A detailed description of the experimental setup and the methods employed to create the dataset is provided by Lopez-Sabater (2001). The experiment was designed so that the resulting database would be representative of overland flow occurring under a wide variety of conditions: different microtopographic configurations, a broad range of slopes, and an extensive selection of flow rates. Five artificial surfaces, 1 m long and 0.5 m wide, with different microtopographic configurations, were constructed using concrete. The surfaces were shaped by hand simulating five different surface conditions, from a smooth plane to a dense network of rills. The goal was not to reproduce natural or man-made surfaces, but to create a collection of appreciably different surfaces. The surfaces were successively coated with sand four times, each time using a larger grain size, thus producing twenty combinations of surface shape and sand cover. The sand was carefully glued to the surface, and when the glue dried, the excess sand was removed.

After the application of a sand cover, each surface was scanned using a laser scanner (Huang and Bradford, 1990) to produce a digital model of the surface microtopography. The scanner was set to record 200 longitudinal profiles 2 mm apart, each one having 900 measurements 1 mm apart. The experimental variogram was computed for each one of the 200 profiles, and later the 200 experimental variograms were pooled together to create an ensemble average. An exponential model was then adjusted using least squares to the variogram ensemble average ( $\gamma_k$ ), and the values of the two model parameters,  $\sigma^2$  [ $L^2$ ] (variance of the elevation measurements) and  $L$  [ $L$ ] (correlation length), were obtained.

The variogram exponential model was (Huang and Bradford, 1992):

$$\gamma_k = \sigma^2(1 - e^{-k/L}) \quad (1)$$

### DATASET

Three parameters were thus used to describe the configuration of the surfaces: the diameter  $d$  of the sand used to coat the surfaces,  $\sigma^2$ , and  $L$ . After the characterization of the microtopography, the surfaces were placed on a flume with a removable central section. The surfaces were positioned so that the flume bed coincided with the surface main plane. The slope of the flume was allowed to vary between 0.5% and 21.1%, and the surfaces were tested for a range of discharges between 0.03 and 0.43  $L m^{-1} s^{-1}$ . Measurements taken from the flume permitted the computation of hydraulic roughness coefficients for different conditions of slope and discharge. Darcy-Weisbach, Manning, and Chezy roughness coefficients were computed from the flume data using the following expressions:

$$f = \frac{8gRS}{V^2} \quad (2)$$

$$n = \frac{1}{V} R^{2/3} S^{1/2} \quad (3)$$

$$C = \frac{V}{\sqrt{RS}} \quad (4)$$

where

- $f$  = dimensionless Darcy-Weisbach roughness coefficient
- $n$  [ $T L^{-1/3}$ ] = Manning's roughness coefficient
- $C$  [ $L^{1/2} T^{-1}$ ] = Chezy's roughness coefficient
- $R$  [ $L$ ] = hydraulic radius
- $S$  [ $L L^{-1}$ ] = flume slope
- $V$  [ $L T^{-1}$ ] = average flow velocity.

The average flow velocity was estimated from measurements of dye clouds. The hydraulic radius was computed by dividing the flow discharge by the average velocity, thus equaling the average depth. Therefore, the roughness coefficients so computed implicitly accounted for the deviation of the actual hydraulic radius from the average depth. Reynolds numbers were computed as:

$$Re = \frac{4VR}{\nu} \quad (5)$$

where  $\nu$  [ $L^2 T^{-1}$ ] = kinematic viscosity.

Eventually, a dataset containing 1827 data records was created. Each record contained a value for each of the following variables:  $d$  (in mm),  $\sigma^2$  (in  $mm^2$ ),  $L$  (in mm), Reynolds number (dimensionless), flume slope (%), Darcy-Weisbach roughness coefficient (dimensionless), Manning roughness coefficient (in  $s m^{-1/3}$ ), and Chezy roughness coefficient (in  $m^{1/2} s^{-1}$ ).

### STACKED NEURAL NETWORK ALGORITHMS

There is no assurance that a single neural network can extract all relevant information from a dataset (Sridhar et al., 1996). It is possible that different neural networks may capture different aspects of the information contained in the dataset, and that aggregating these networks can improve the

estimation of roughness coefficients. Stacked neural network algorithms were created as combinations of 100 neural networks, with the overall output being the average of the individual network outputs. The outputs of the individual networks were restricted to the range of roughness coefficients measured in the flume experiment. Network outputs outside that range were set equal to the maximum or minimum of the measured values.

In order to develop the neural networks, the dataset was divided in three subsets. First, 20% of the dataset records were randomly selected and separated from the rest. This subset constituted the testing set and eventually was used to test the predictive capabilities of the algorithms. The remaining 80% of the dataset was divided into a training set, consisting of 60% of the records and used to calibrate the neural networks, and a validation set. The purpose of the validation set was to stop the calibration process soon enough to avoid overfitting. Overfitting occurs when the network being calibrated attempts to account for features in the input variables that are of progressively lesser significance, and which indeed may represent information unrelated to the investigated relationship. Such features can be considered to be noise in the context of the pattern being sought. When overfitting occurs, the error on the training set is driven to a very small value, but when new data is presented to the network, the error is large. In this case, the network has memorized the training examples, but it has not learned to generalize to new situations (Rzempoluck, 1998).

Training and validation sets were randomly resampled for each of the neural networks, thus ensuring that the dataset used to calibrate each network was somewhat different from the sets used to calibrate the rest of the networks in the stack. The parameters of each neural network (weights and biases) were obtained in an iterative calibration procedure based on the Levenber-Marquardt algorithm (Demuth and Beale, 1998) and the minimization of the mean squared error (MSE) objective function. The procedure was repeated 100 times to generate 100 networks. Each network was then evaluated in terms of the MSE for both the training and validation sets. Those networks with an MSE larger than two times the average of the 100 networks were discarded and replaced with new networks.

In modeling neural networks, it is difficult to specify *a priori* the optimum network architecture. Demuth and Beale (1998) suggested that a feed-forward back-propagation neural network, with one nonlinear hidden layer and a linear output layer, can approximate any unknown relationship with a finite number of discontinuities, given sufficient neurons in the hidden layer. The number of nodes in the hidden layer depends on the complexity of the underlying problem and is determined empirically by calibrating and testing different architectures. In this study, five network architectures were tested using, as recommended by Demuth and Beale (1998), a single sigmoidal hidden layer and a linear output layer as the basic scheme. The network architectures differed only in the number of nodes in the hidden layer (4, 8, 12, 16, or 20), which in turn determined the total number of parameters that the calibration procedure would have to adjust (29, 57, 85, 113, or 141). Large network architectures cause the training process to last significantly longer and can induce overfitting, which translates into a loss of generalization ability and an increase in estimate errors for records not included in the training set.

## EVALUATION CRITERIA

The purpose of evaluation is to verify that the identified models fulfill a series of requirements according to objective criteria for good model approximation. It is usually a major objective to obtain a model of least possible complexity within the limits of required model accuracy. The residuals of a model represent the misfit between measured data and model outputs. The presence of any information remaining in the residuals is an indication that the model might be insufficiently complex or otherwise inappropriate (Martin and Morris, 1999).

The stacked neural network algorithms were evaluated using the subset reserved for testing purposes, which consisted of 20% of the records in the original dataset that were not used in the development and calibration of the neural networks. The input variables of each testing record were presented to the stacked algorithms and used to estimate a roughness coefficient. The performance of the algorithms was then evaluated in terms of the root square of the residuals (RMSR) and the correlation coefficient ( $r$ ) between observed and predicted roughness coefficients. The root mean square of the residuals was computed using the expression:

$$\text{RMSR} = \sqrt{\frac{\sum_{i=1}^N (O_i - P_i)^2}{N}} \quad (6)$$

where

$O$  = "observed" roughness coefficients (calculated from the flume measurements)

$P$  = predicted values (neural network algorithm outputs)

$N$  = number of observations in the testing subset.

Another index used in evaluating the models was the final prediction error (FPE) (Martin and Morris, 1999), which was computed using the formula:

$$\text{FPE} = \frac{E}{2N} \left( \frac{N + N_w}{N - N_w} \right) \quad (7)$$

where

$E$  = average squared error over the  $N$  data points

$N_w$  = number of adjustable parameters or weights in each network.

To compute the index FPE, the value of  $E$  was substituted with the squared value of the RMSR. The objective of the modeling approach is to reach a balance between the accuracy of model fit and the number of parameters, and minimization of this test function leads to networks that are neither under- nor over-complex.

If the model is correct, then the residuals should be structureless. In particular, they should be uncorrelated with any other variables, including inputs and outputs. A simple check is to plot the residuals versus the output values. Such a plot should not reveal any obvious pattern. Another valuable diagram is the histogram of the residual amplitudes, which reveals distributions that differ from the normal distribution.

Finally, a sensitivity analysis was performed to test the prediction ability of the stacked models within the whole range of variability of the input variables. A base data record was created averaging the maximum and minimum values of the input variables. Then two of the input variables were

allowed to vary between their minimum and maximum values, while the other three were kept constant at their base values. The new combinations of input variables were presented to the stacked network models to predict the roughness coefficients associated with the new records. For each model, the procedure was repeated ten times to allow all possible pairs of input variables to vary at a time. Model estimates were assembled in surface plots with the two horizontal axes corresponding to the two input variables that were allowed to change in the analysis.

## RESULTS AND DISCUSSION

Figure 1 presents the values of the RMSR for each of the 100 neural networks that make up three of the algorithms developed, as well as the evolution of the RMSR when the networks were added one at a time to create the stacked models. The figure depicts the case of networks with 12 hidden nodes. Plots a, c, and e show the RMSR for the individual networks, while b, d, and f show the effect of progressively combining the networks in stacked models. It is apparent that the predictive ability of each network is different from the rest, and that combining the networks in a single model reduces the overall RMSR (e.g., fig. 1b) and integrates all the learning done by the individual networks. The selected number of networks (100) looks reasonable and is similar to the number of networks selected in other studies (Schaap et al., 1998). Evidence from this study suggests that increasing the number above 100 does not significantly alter the overall RMSR. Results presented in the following sections refer to the stacked neural network algorithms.

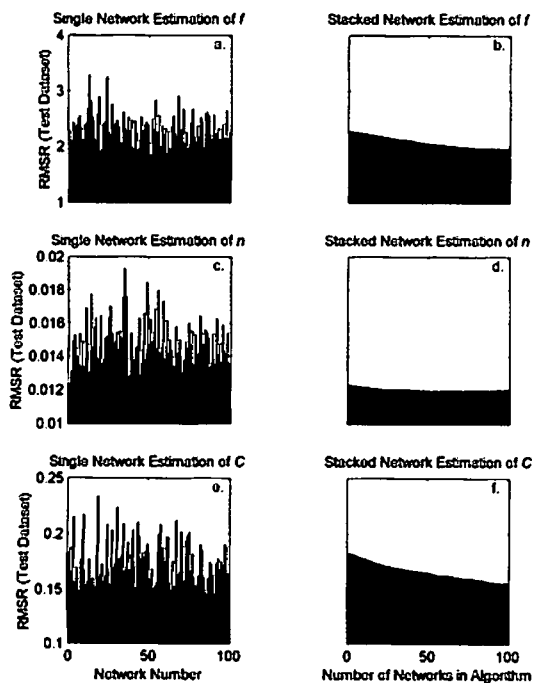


Figure 1. RMSR (root mean square of the residuals) of single neural networks for Darcy-Weisbach's  $f$ , Manning's  $n$ , and Chezy's  $C$  with 12 hidden nodes and the stacked algorithms for records in the testing data subset.

## PREDICTIONS VS. OBSERVATIONS: CORRELATION COEFFICIENTS

Estimates based on the input variables of the testing records were compared to their corresponding flume measurements. Correlation coefficients between observations and estimates were computed and are shown in figure 2. In all cases, the values of  $r$  are above 0.90, which gives an idea of the quality of the model predictions for input data obtained from the laboratory experiment. It is also apparent from figure 2 that increasing the complexity of the neural networks (i.e., the number of neurons in the hidden layer) causes an improvement in model predictions. The rate of improvement is larger for models of low complexity. As complexity increases (12 neurons or more in the hidden layer), the performance evaluated as the correlation coefficient does not improve much more.

There is also a clear ranking in model performance that responds to the type of roughness coefficient predicted. Models predicting Chezy roughness coefficients produced the highest correlation coefficients for network algorithms with any number of hidden nodes. In addition, algorithms predicting Manning roughness coefficients produced correlation coefficients higher than algorithms predicting Darcy-Weisbach coefficients. This difference in performance might be associated with the different relationship that the roughness coefficients display with the Reynolds number.

Figure 3 shows how different the distributions of the three roughness coefficients were based on flume measurements at approximately constant Reynolds number ( $Re$ ) intervals. Chezy coefficients obtained from the flume experiment were linearly related to  $Re$ , while Manning and especially Darcy-Weisbach coefficients were linearly related to the logarithm of  $Re$ . The logarithmic relation to  $Re$  caused most of the Darcy-Weisbach roughness coefficients obtained from the flume experiment, and many of the Manning coefficients,

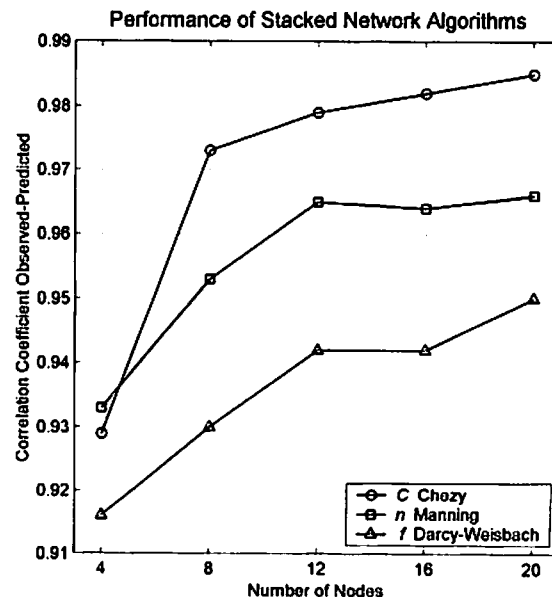


Figure 2. Correlation coefficients between observed and predicted roughness coefficients versus neural network complexity (number of nodes in the hidden layer).

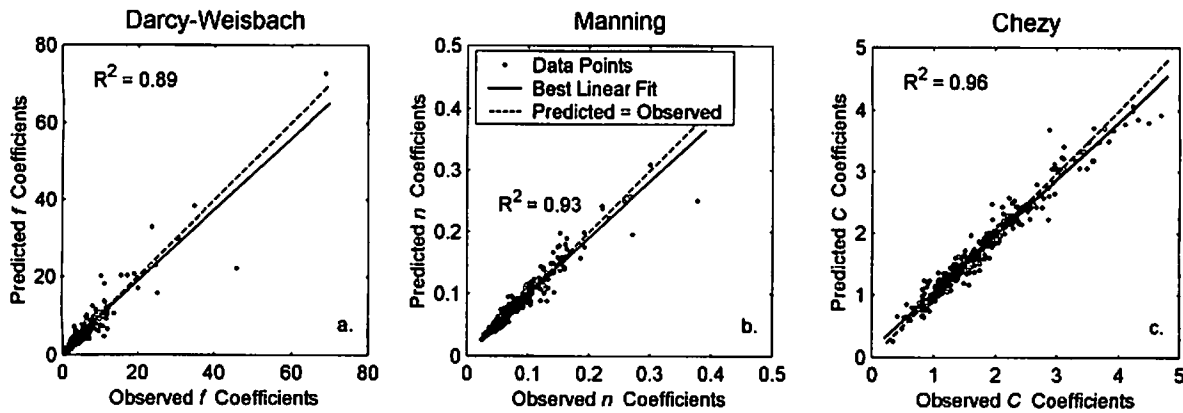


Figure 3. Performance of stacked models of neural networks with 12 nodes in the hidden layer.  $R^2$  is the coefficient of determination of the best linear fit.

to be relatively small (see fig. 3), therefore creating an asymmetric dataset. Trained with this dataset, the neural networks learned to predict small coefficients better than large coefficients, and consequently, the errors associated with prediction of large coefficients in the testing dataset are larger for Darcy–Weisbach networks than for Manning networks, and larger for Manning networks than for Chezy networks.

#### RMSR AND FPE

The second index used to compare model performance was the root mean square of the residuals, which was computed using equation 6. Figure 4 shows the same tendencies observed in figure 2, that is, RMSR decreases monotonically with increasing model complexity, and the rate of improvement declines with the number of nodes in the hidden layer.

The final prediction error (FPE) index balances the accuracy of the model estimates and the algorithm complexity, and therefore can be used to identify the optimal model

architecture. Figure 5 shows the FPE values produced by the different models versus complexity (i.e., the number of hidden nodes). The decreasing tendency previously observed for the RMSR has been counterweighted by the effect of the number of parameters. All three models seem to show a minimum FPE value, and therefore an optimum architecture, within the range of hidden nodes tested. The Darcy–Weisbach algorithms have a minimum FPE for networks with 4 to 12 nodes, the Manning algorithms have a minimum FPE for networks with 12 nodes, and the Chezy algorithms appear to have a minimum FPE for networks with 12 to 20 nodes. Again, the difference in optimum network architecture might be connected to the relationship of the roughness coefficients to the Reynolds number.

All Darcy–Weisbach networks learned to reproduce small roughness coefficients better than large roughness coefficients. Simple networks learned to reproduce small coefficients to a high degree of accuracy because records in this class were abundant in the training dataset, but not even the most complex networks (i.e., with 20 hidden nodes) were

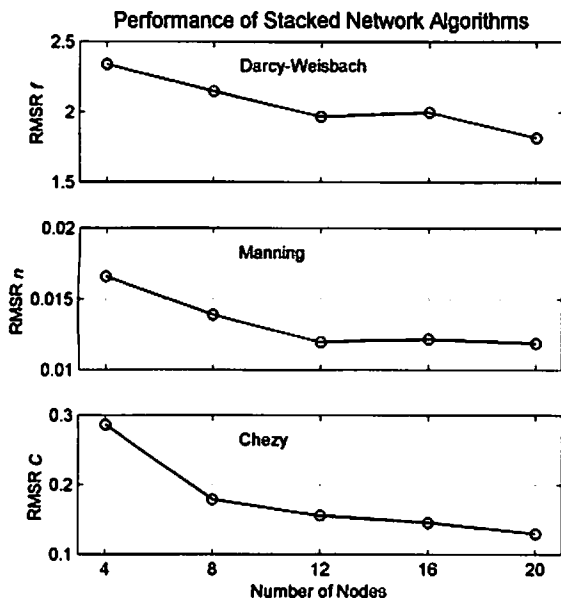


Figure 4. RMSR versus model complexity (number of nodes in the hidden layer of the networks used to create the stacked algorithm) for the testing data subset.

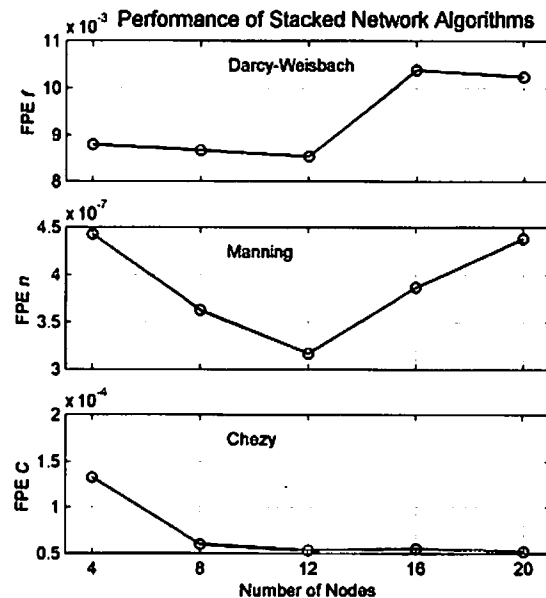


Figure 5. FPE (final prediction error) versus model complexity (number of nodes in the hidden layer of the networks used to create the stacked algorithm) for the testing data subset.

able to accurately reproduce large coefficients because of the lack of records from which to learn the relationship. Consequently, all the networks produce large errors when they are used to reproduce large coefficients, and therefore little improvement is achieved when the network complexity is increased. On the other hand, Chezy networks learned to reproduce roughness coefficients of all magnitudes because all were equally abundant in the training dataset. Increasing the complexity of the networks was worthwhile in this case because it was compensated by a significant improvement in information extraction. Manning networks clearly represent an intermediate situation.

### RESIDUALS

Results from the analysis of residuals for the algorithms based on 12-node networks are shown in figure 6. Plots a, c, and e are histograms of the residuals, while plots b, d, and e show the residuals versus the measured roughness coefficients. In all cases, the histograms of the residuals were centered at zero and displayed a normal-shaped distribution. The residuals did not show any pattern when plotted against the measured roughness coefficients, although the magnitude of the residuals did increase with the values of the coefficients for Darcy-Weisbach and Manning. These results reflect again the high degree of accuracy of the stacked models when they were used to predict the roughness coefficients measured from the laboratory experiment.

### SENSITIVITY ANALYSIS

A base data record was created as the average of the maximum and minimum values of the input variables in the dataset. The base values of the input variables were:  $d = 1.78$  mm,  $\sigma^2 = 40.4$  mm<sup>2</sup>,  $L = 100$  mm,  $Re = 710$ , and  $S = 11.5\%$ . Figure 7 shows the response surfaces generated with the Darcy-Weisbach algorithm based on networks with 8 neurons in the hidden layer as an example. These surfaces have been created by restricting the output of the individual

neural networks to a limited range of  $f$  values (0.36 to 90.8). This artifact prevents outliers but does not affect the overall shape of the surface.

One important characteristic of the surfaces is their smoothness. None of the surfaces show sudden changes of magnitude or trend for small changes of the input variables, as can be the case for single neural networks. This suggests that the stacked network algorithm has been able to learn the underlying relationship between input variables and roughness coefficients. Furthermore, the stacked models were able to generalize what was learned from the training records to other combinations of input variables.

Interpretation of the response surfaces is difficult and can be done only to a limited extent. In general, friction tends to decrease both with slope and with Reynolds number. Increasing slopes cause flow concentration in microtopographic depressions and a consequent reduction of friction. Increasing discharge, and therefore Reynolds number, produces an increase in hydraulic radius and submergence of roughness particles, thus causing a decline in roughness coefficients. The effect of the sand diameter is small compared with the other variables, and its contribution to the roughness coefficients is generally masked by the other factors.

The contributions of  $\sigma^2$  and  $L$  are the most difficult to interpret. Both factors appear to have a large influence in roughness coefficients for small slope and Reynolds number. When slope or Reynolds number increase, the effects of both  $\sigma^2$  and  $L$  are damped out and friction losses decrease. Significantly, both variables cause the predicted roughness coefficient to peak within their range of variability. The peak occurs for a  $\sigma^2$  of about 30 mm<sup>2</sup> and  $L$  of about 100 mm. For

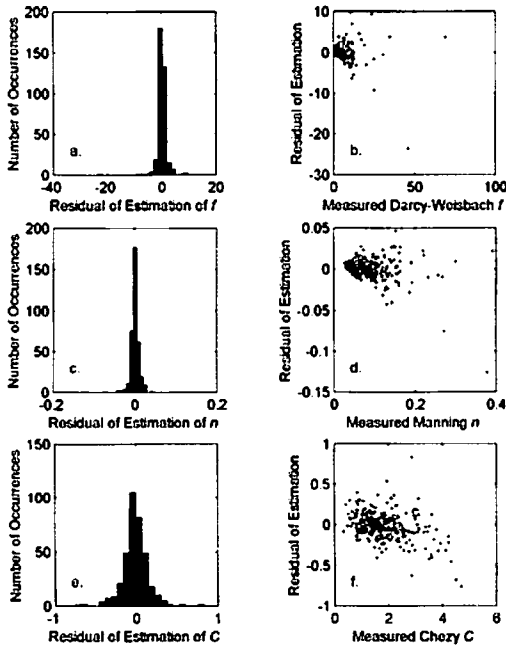


Figure 6. Evaluation of the residuals for algorithms with networks with 12 hidden nodes.

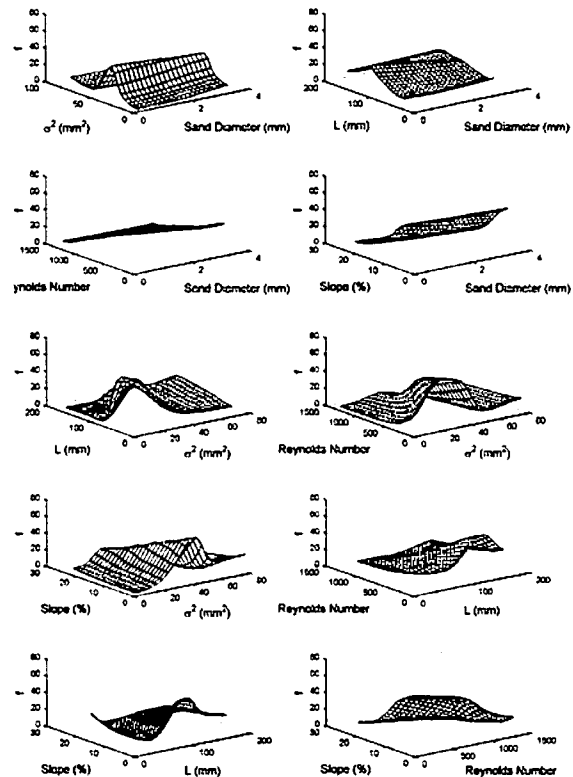


Figure 7. Sensitivity analysis of the Darcy-Weisbach algorithm based on networks with 8 hidden nodes.

the surfaces tested in the flume experiment, the value of  $\sigma^2$ , the variance of the elevation measurements, was small for flat surfaces and increased with larger microtopography. The larger values corresponded to the rilled surfaces, which restricted flow to the bottom of the microtopographic depressions. This can explain the initial rise and subsequent decrease of roughness coefficients for  $\sigma^2$ . However, the values of  $L$  are related to the spatial correlation of the elevation measurements, rather than to the degree or size of the roughness elements. This fact makes the interpretation of the influence of  $L$  more difficult.

Similar response surfaces were generated with the Manning and Chezy algorithms, with network outputs limited to the range 0.027 to 0.48 s m<sup>-1/3</sup> for Manning networks and to the range 0.20 to 4.69 m<sup>1/2</sup> s<sup>-1</sup> for Chezy networks.

## CONCLUSIONS

This study presents a method for combining relatively simple neural networks into a stacked algorithm to generate reliable estimates of hydraulic roughness coefficients from measurable data. The following conclusions can be drawn based on the development of the neural network algorithms and testing results:

- Combining neural networks in a stacked algorithm reduced the RMSR of the predictions. As networks are combined into the stacked algorithm, the RMSR becomes increasingly smaller. The RMSR of the stacked algorithm was always similar to (slightly larger or slightly smaller than) the RMSR of the best neural network.
- The experimental sampling scheme created an asymmetric dataset of Darcy–Weisbach and Manning coefficients that prevented the neural networks from adequately learning the relationship between input and output variables.
- Increasing network complexity (i.e., number of nodes in the hidden layer) caused the RMSR of the stacked algorithm to decrease and the correlation between predictions and observations to increase. However, the rate of improvement diminished when the network complexity increased. The FPE index can be used to identify the optimum neural network architecture, which is dependent on the complexity of the underlying relationship and the quality of the dataset.
- Residuals from the stacked neural network algorithms were normally distributed and no clear trend between residuals and estimated roughness coefficients was observed.
- The response surfaces generated in the sensitivity analysis were smooth. The stacked algorithms were able to reproduce the relationships between input variables and roughness coefficients in the training dataset, and learned to generalize these relationships to other combinations of input variables.

## ACKNOWLEDGEMENTS

This research was partially supported by the *Comisión Interministerial de Ciencia y Tecnología (CICYT)* of Spain. The authors are also grateful to Dr. Chi–Hua Huang for providing the laser scanner and for his advice.

## REFERENCES

- Abrahams, A. D., A. J. Parsons, and S. H. Luk. 1990. Field experiments on the resistance to overland flow on desert hillslopes. In *Erosion, Transport, and Deposition Processes*, 1–18. Proceedings of the Jerusalem Workshop, March–April 1987. IAHS Publ. No. 189. Oxfordshire, U.K.: International Association of Hydrological Sciences.
- Demuth, H., and M. Beale. 1998. *Neural Network Toolbox User's Guide*. Natick, Mass.: The MathWorks, Inc.
- Emmett, W. W. 1970. The hydraulics of overland flow on hillslopes. USGS Professional Paper 662–A. Reston, Va.: U.S. Geological Survey.
- Fiedler, F. R., and J. A. Ramirez. 2000. A numerical method for simulating discontinuous shallow flow over an infiltrating surface. *Int. J. Numer. Meth. Fluids* 32(2): 219–240.
- Gandolfi, C., and F. Savi. 2000. A mathematical model for the coupled simulation of surface runoff and infiltration. *J. Agric. Eng. Res.* 75(1): 49–55.
- Govindaraju, R. S., M. L. Kavvas, and G. Tayfur. 1992. A simplified model for two–dimensional overland flows. *Advances in Water Resources* 15(2): 133–141.
- Huang, C., and J. M. Bradford. 1990. Portable laser scanner for measuring soil surface roughness. *Soil Sci. Soc. Am. J.* 54(5): 1402–1406.
- \_\_\_\_\_. 1992. Applications of laser scanner to quantify soil microtopography. *Soil Sci. Soc. Am. J.* 56(1): 14–21.
- Lopez–Sabater, C. J. 2001. An empirical model of hydraulic roughness for overland flow. PhD diss. Tucson, Az.: University of Arizona, Department of Agricultural and Biosystems Engineering.
- Martin, E. B., and A. J. Morris. 1999. Artificial neural networks and multivariate statistics. In *Statistics and Neural Networks: Advances at the Interface*, 195–257. J. W. Kay and D. M. Titterton, eds. Oxford, U.K.: Oxford University Press.
- Rauws, G. 1988. Laboratory experiments on resistance to overland flow due to composite roughness. *J. Hydrol.* 103(1–2): 37–52.
- Rzempoluck, E. J. 1998. *Neural Network Analysis Using Simulnet*. New York, N.Y.: Springer–Verlag.
- Schaap, M. G., F. J. Leij, and M. T. Van Genuchten. 1998. Neural network analysis for hierarchical prediction of soil hydraulic properties. *Soil Sci. Soc. Am. J.* 62(4): 847–855.
- Shayya, W. H., and S. S. Sablani. 1999. Use of artificial neural networks in the noniterative calculation of the friction coefficients in closed pipe and open channel flow. Presented at the 1999 ASAE/CSAE–SCGR Annual International Meeting. Paper No. 993011. St. Joseph, Mich.: ASAE.
- Sridhar, D. V., R. C. Seagrave, and E. B. Barlett. 1996. Process modeling using stacked neural networks. *AIChE J.* 42(9): 2529–2539.
- Zhang, W., and T. W. Cundy. 1989. Modeling of two–dimensional overland flow. *Water Resources Res.* 25(9): 2019–2035.